Reaction of Benzene and Boron Atom: Mechanism of Formation of Benzoborirene and Hydrogen Atom

Holger F. Bettinger*,† and Ralf I. Kaiser*,‡

Lehrstuhl für Organische Chemie II, Ruhr-Universität Bochum, Universitätsstrasse 150, 44780 Bochum, Germany, and Department of Chemistry, University of Hawai'i at Manoa, Honolulu, Hawaii 95622

Received: November 19, 2003; In Final Form: February 12, 2004

The reaction of C_6D_6 + B(^{2}P) is investigated by crossed molecular beam experiments at a collision energy of 5.5 kcal mol^{-1} and by electronic structure computations. The latter were performed employing hybrid Hartree−Fock/density functional theory (B3LYP), coupled cluster theory with single, double, and a perturbative estimate of triple excitations [CCSD(T)], complete active space self consistent field (CASSCF), and multiconfiguration quasi-degenerate perturbation theory to second order (MC-QDPT2) in conjunction with 6-31G*, 6-311+G**, and cc-pVTZ basis sets. Final energies were obtained at the CCSD(T)/cc-pVTZ//B3LYP/6-311+G** + ZPVE level of theory. Two possible addition channels to the benzene π system were characterized. One involves a weakly bound benzene−boron π complex and proceeds over a barrier, which lies below the energy of separated reactants, to an η_1 $C_6H_{6-}B$ σ complex (**4**). The second channel is the symmetric attack (η_2) to a π bond of benzene. This addition mode following the ^{2}A″ potential energy surface involves a valley ridge inflection (VRI) point and therefore results in **4**. This VRI point also makes the formation of the 7-boranorbornadiene-7-yl radical (**6**, ^{2}A′) via nonadiabatic transition from ^{2}A″ to ^{2}A′ unlikely. The primary addition products **4** (and **6**) can rearrange over barriers below the energy of separated reactants to finally reach the phenylboryl radical (**10**, ^{2}A′). This is the most stable C_6H_6B species identified. Cleavage of an *o*-CH bond goes along with closure of a C−B bond and yields benzoborirene (**1**, ^{1}A$_1$) and hydrogen atom (−19.2 kcal mol^{-1}; −16.7 kcal mol^{-1} for the [D_6]-benzene system). Abstraction of hydrogen by boron to produce phenyl radical (^{2}A$_1$) and borylene ($^1\Sigma^+$) is endoergic by +30.4 kcal mol^{-1} (C_6D_5 + BD, +31.6 kcal mol^{-1}) and is therefore not viable under our experimental conditions. The features of this C_6D_6B potential energy surface identified computationally—no entrance barrier with respect to separated reactants, exoergicity of −16.7 kcal mol^{-1}, transition state energy and structure in the exit channel (6.5 kcal mol^{-1} with respect to **1** + D)—are in agreement with crossed-beam data (exoergicity −14.8 ± 1.2 kcal mol^{-1}; exit channel barrier 2.4−4.8 kcal mol^{-1}). Phenylborylene **2** and didehydroborepine **3** are alternative C_6H_5B species, but these are higher in energy than **1** by 32 and 43 kcal mol^{-1} and are therefore not formed in the crossed-beam experiment.

Introduction

Employing matrix isolation IR spectroscopy, the reactions of boron atoms with methane,[1−5] acetylene,[6−8] ethylene,[9] ethane,[9] and methanol[10,11] have been investigated, while the dynamics of reactions of boron atoms with ethylene,[12,13] acetylene,[14] and dimethylacetylene[15] have been probed utilizing the crossed-beam technique. We have recently reported that the reaction of boron atoms with deuterated benzene, C_6D_6, results in the formation of C_6D_5B and a deuterium atom under the single collision conditions of a crossed molecular beam apparatus as indicated by time-of-flight mass spectrometry.[16] By comparing the experimental and computed reaction energies for possible C_6D_5B products as well as geometric and energetic data for the transition state in the exit channel, we concluded that [D_5]-benzoborirene ([D_5]-**1**) was the reaction product observed in this experiment. Other possible C_6D_5B reaction products considered, phenylborylene ([D_5]-**2**) and the didehydroborepine isomer ([D_5]-**3**), were found to be much higher in energy than **1** and thus could be excluded as reaction products. While **1** has been repeatedly studied with respect to the Mills−Nixon effect,[17−19] **2** was sought experimentally in 1970 by Fox et al.[20] The 1-naphthyl analogue (also called 1-naphthylboryne) of phenylborylene **2** was reported in 1977 to result from irradiation (λ > 350 nm) of tri-1-naphthylboron in solution,[21] but this claim was refuted 7 years later.[22] The only theoretical investigation of **2** has been reported by Uddin et al.,[23] who studied its bonding properties in transition metal compounds, while **3** has never been studied before to the best of our knowledge.

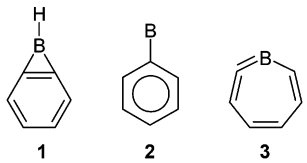

1 **2** **3**

The valence-isoelectronic Al−benzene system has received some attention earlier. Matrix isolation ESR[24,25] and gas-phase time-resolved resonance fluorescence spectroscopy[26] indicate

* Corresponding authors. Fax: +49-234-321-4353; e-mail: Holger.Bettinger@rub.de (H.F.B.).
† Ruhr Universität Bochum.
‡ University of Hawai'i at Manoa.

10.1021/jp0375259 CCC: $27.50
Published on Web 05/05/2004

that a η^2-C_6H_6−Al species is formed with a binding energy of 11.7 ± 1 kcal mol^{-1}. Computational investigations[27,28] support the assignment of the observed species to a norbornadiene-like system with a transannular aluminum bridge. However, single-collision crossed-beam data are not available for the Al−C_6H_6 system.

In this paper we report a detailed computational and experimental investigation of the reaction of benzene with a boron atom. We consider the entrance and exit channels of the reaction as well as rearrangements of C_6H_6B species. The information thus gained, along with data from crossed-beam experiments described here, allows the identification of the lowest energy pathway for formation of benzoborirene + H from the reactants.

Theoretical Details

The geometries of stationary points were optimized using Becke's[29] three-parameter hybrid density functional as implemented[30] in the Gaussian[31] program in conjunction with the exchange functional of Lee, Yang, and Parr[32] (B3LYP). A finer integration grid (99 radial shells and 590 angular points per shell) was used for a number of structures with low (imaginary) vibrational frequencies (**3**-^{3}A′, **4**-C_s/**4**-C_1, $\mathbf{6_E}$-^{2}A′, **13**), but in all cases no qualitative difference was observed. Intrinsic reaction coordinates (IRC) were computed for selected transition states with the Gonzalez−Schlegel algorithm.[33,34]

The energies of selected stationary points were refined by single point energy computations utilizing coupled cluster theory with single, double, and a perturbative estimate of triple excitations [CCSD(T)][35,36] in conjunction with Dunning's[37] correlation consistent cc-pVTZ basis set. The partially spin projected algorithm was used for open-shell species [RHF-RCCSD(T)].[36,38] All CCSD(T) computations were performed with MOLPRO.[39]

We decided to investigate parts of the C_6H_6B potential energy surface (PES) with complete active space self consistent field (CASSCF) theory. The following active spaces were employed: (i) ten orbitals (six π/π^* and the four atomic orbitals (AOs) on boron) and nine electrons (six π of benzene, three of boron) for investigations of the entrance channels, the primary addition products (**4** and **5**), and the transition state (**TS1**) for CH insertion; (ii) eight orbitals (seven π and 1s of H) and seven electrons (six π and one electron of the hydrogen atom) for the transition state for H atom addition to benzoborirene (**1**). Geometry optimizations with the (9,10)- and (7,8)-CASSCF wave functions employed the 6-31G* basis set.[40] Harmonic vibrational frequencies were computed by finite differences of analytic gradients. The energies were refined by single point computations using multiconfiguration quasidegenerate perturbation theory to second order (MC-QDPT2)[41,42] and the cc-pVTZ[37] basis set with the same active spaces as used in the respective geometry optimizations. These multiconfiguration computations were performed using the GAMESS program.[43]

Unless noted otherwise, the energies mentioned in the text were obtained at the CCSD(T)/cc-pVTZ//B3LYP/6-311+G** level of theory including unscaled zero-point vibrational energy (ZPVE) corrections.

Experimental Details

Helium-seeded boron atoms were generated in the gas phase via laser ablation of a boron rod; this beam crossed a second beam of [D_6]-benzene seeded in argon perpendicularly in a scattering chamber at a collision energy of 5.5 ± 0.2 kcal mol^{-1}. A rotatable quadrupole mass spectrometer coupled to an electron impact ionizer analyzed the reaction product via the time-of-flight (TOF) technique.[16,44] TOF spectra were recorded at distinct angles; an integration of these spectra led to the laboratory angular distribution. A forward-convolution technique was utilized to transform the laboratory data into the center-of-mass reference frame. This procedure yields the center-of-mass translational energy, $P(E_T)$, and the angular distributions, $T(\theta)$.

Results and Discussion

Stationary points discussed in this paper are displayed in Figures 1 and 2.

A. Entrance Channels and Their Primary Products. *Addition to the Benzene π System.* Orbital symmetry considerations are very helpful in characterizing the possible addition modes of boron atom to benzene. A complex between a boron atom, $(2s)^2$ $(2p)^1$, centered over a benzene molecule in C_{6v} symmetry ($2p_z$, a_1; $2p_{x,y}$, e_1) can have a $^2A_1$ or a $^2E_1$ electronic state. The degenerate open-shell $^2E_1$ state is subject to a first-order Jahn−Teller distortion. The two degenerate $2p_x$ and $2p_y$ orbitals transform according to b_2 and b_1 irreducible representations in C_{2v} symmetry (the $2p_z$ AO still belongs to a_1), while the benzene π^* orbitals belong to a_1 and a_2. Further lowering of symmetry to C_s is thus necessary, and this can proceed in two ways (Figure 3): (i) the σ_{xz} symmetry plane is preserved, resulting in **4** by attack at the benzene *corner*, or (ii) the σ_{yz} symmetry plane is preserved, resulting in **5** by attack at the benzene *edge*. The $^2A_1$ state is higher in energy than $^2E_1$ at intermediate distances due to enhanced repulsive interaction among the seven electrons. However, within A_1 state symmetry, the transannular addition product **6**-C_{2v} (Figure 3) correlates with the reactants.

Let us now consider the properties of the primary addition products **4**−**6**. The electronic state of the *corner* addition product, **4**, is $^2A'$ in C_s symmetry. We find **4**-C_s to be a minimum at the (9,10)-CASSCF/6-31G* level of theory. The singly occupied molecular orbital (SOMO) is the π_3 of cyclohexadienyl, while boron has a lone pair and two empty p-type orbitals. On the other hand, an imaginary vibrational frequency (67i cm^{-1}, a″) is obtained at B3LYP/6-311+G**, also using the finer integration grid. An asymmetric structure **4**-C_1 is found to be more stable by 0.07 kcal mol^{-1} (B3LYP) or 0.03 kcal mol^{-1} [CCSD(T)]. The electronic configuration of **4**-C_1 is similar to that of **4**-C_s. The **4**-C_1 structure is characterized by a B−C−C angle of 88.0°, indicative of a hyperconjugative interaction between one of the vacant orbitals on B and a C−C bond. The C(B)−C bond participating in hyperconjugation in **4**-C_1 is 0.012 Å longer than the other one, while the C−B distance in **4**-C_1 is 0.017 Å longer than in **4**-C_s. The structures of related alkyl carbenes, which can be stabilized by hyperconjugation,[45−47] also depend strongly on the inclusion of dynamic correlation.[48] However, **4**-C_s is lower in energy than **4**-C_1 by 0.1 kcal mol^{-1} after inclusion of ZPVE corrections. The zero-point averaged structure may therefore be effectively of C_s symmetry. Relative to the reactants, **4**-C_s is bound by 8.6 or 9.4 kcal mol^{-1} (B3LYP/6-311+G**).

The addition product (**5**, $^2A''$) to the benzene edge is characterized by a SOMO of a″ symmetry, which involves a bonding interaction between boron and the two nearest carbon atoms (Figure 4), and by an electron lone pair at boron. However, **5** is not a minimum at the B3LYP and (9,10)-CASSCF/6-31G* levels, but is a transition state for rearrangement of the B atom on the periphery of the benzene molecule with **4** being the corresponding minimum.

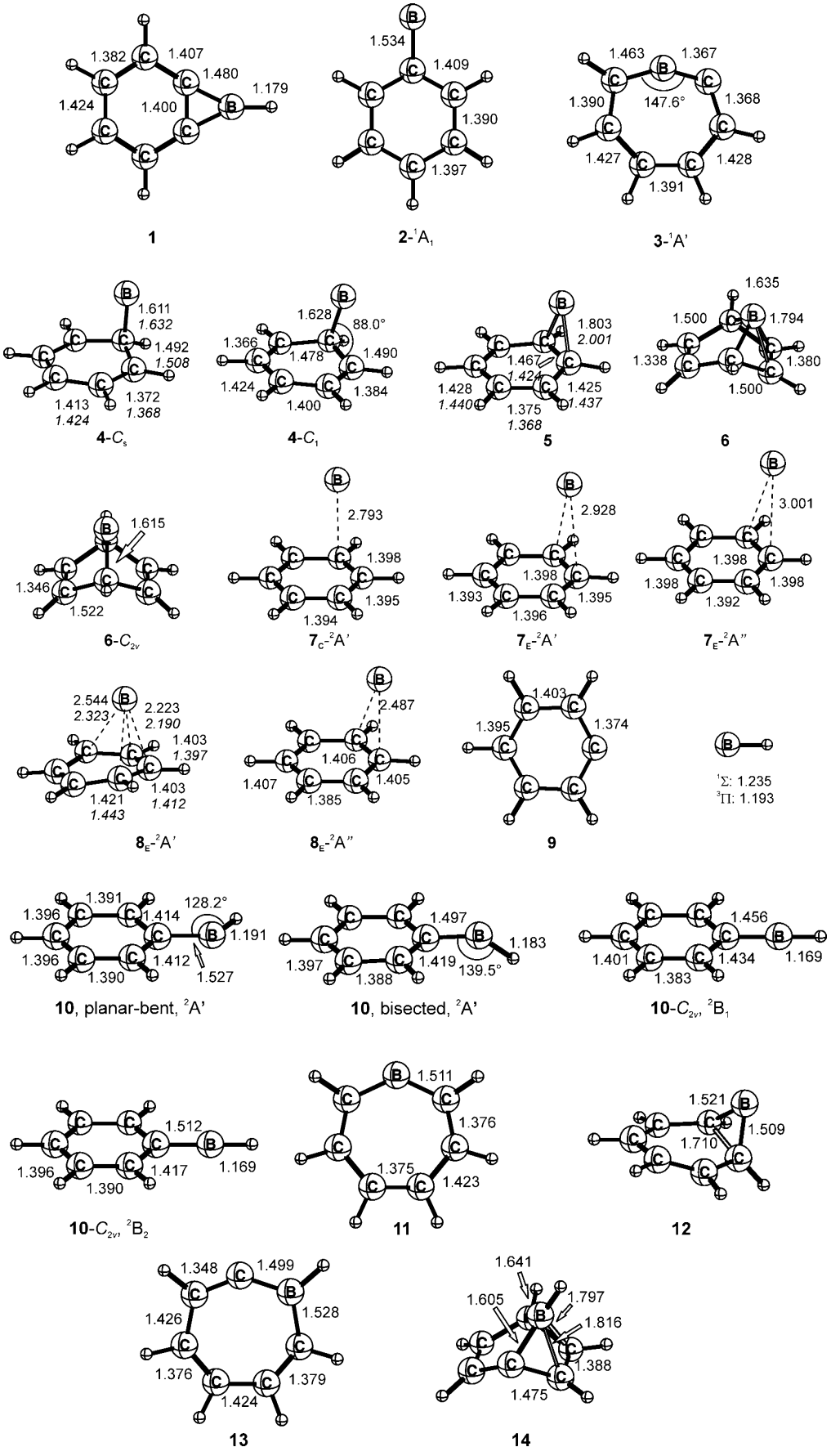

Figure 1. Geometries of stationary points as computed at the B3LYP/6-311+G** level of theory. Where available, (9,10)-CASSCF/6-31G* data are given in italics. All bond lengths are given in angstroms; bond angles are given in degrees.

The 0.5 kcal mol^{-1} barrier for this rearrangement through **5** is considerably lower than that for protonated benzene, $C_6H_7^+$. There, the bridged structure lies about 6−10 kcal mol^{-1} above the C_s symmetric σ complex.[49,50]

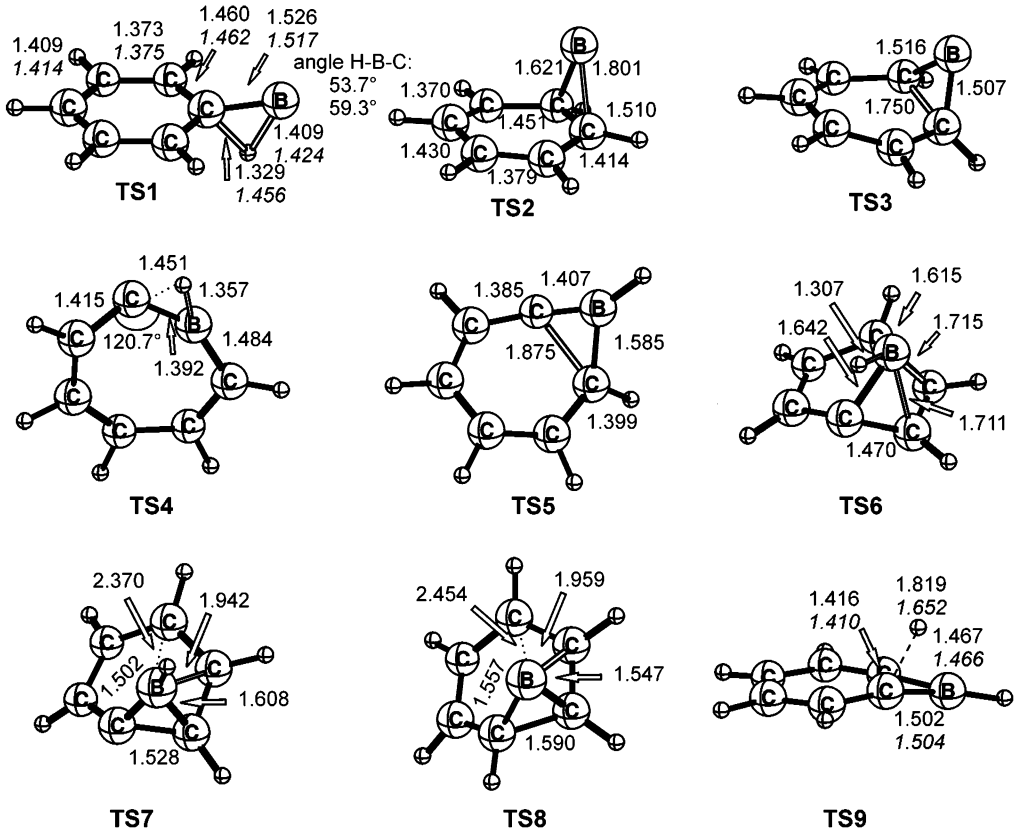

Figure 2. Geometries of transition states on the C_6H_6B potential energy surface as computed at the B3LYP/6-311+G** level of theory. Where available, CASSCF/6-31G* data are given in italics. All bond lengths are given in angstroms; bond angles are given in degrees.

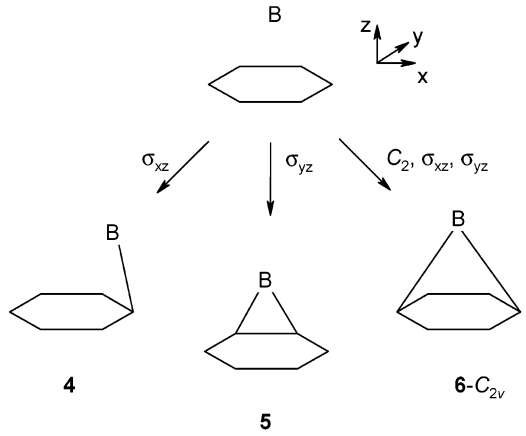

Figure 3. Schematic representation of addition of boron atom to benzene molecule within C_s and C_{2v} symmetries resulting in corner (**4**), edge (**5**), and transannular (1,4) addition (**6**-C_{2v}) products.

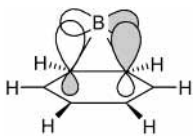

Figure 4. Schematic representation of singly occupied molecular orbital (a″ symmetry) of benzene−boron atom complex **5**.

The transannular addition product **6**-C_{2v} is not a minimum (335i cm^{-1}, b_1) either: tilting the boron atom toward one of the C═C double bonds lowers the energy. This indicates a homoconjugative stabilization of the boron center by the neighboring C═C double bond in the minimum **6** of C_s symmetry.[51] The latter is the boron-centered radical derived from 7-boranorbornadiene, **6**-H, which has been studied computationally by Schulman et al.[51] The barrier for flipping of the boron atom bridge to the other C═C bond through **6**-C_{2v} is only 7.8 kcal mol^{-1} (Scheme 1). This barrier is somewhat lower than the 15.8 kcal mol^{-1} obtained by Schulman et al.[51] for **6**-H at the MP2(full)/6-31G*//HF/6-31G* level.

SCHEME 1: Degenerate Bridge Flipping in 7-Boranorbornadiene-7-yl (6) through the C_{2v} Symmetric Transition State 6-C_{2v}

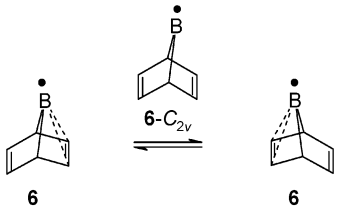

Having characterized possible products of addition to the benzene π system, we now consider the reaction paths connecting these addition products to separated reactants in order to elucidate details of their formation mechanisms. Long-range complexes are given the label **7** while maxima on potential energy curves are **8**. To distinguish between *corner*, *edge*, and C_{2v} attack, we use "C," "E," and "C_{2v}" subscripts in conjunction with **7** and **8**. We begin our analysis with the attack of boron at the *corner* of benzene preserving the σ_{xz} mirror plane. This is the most straightforward mechanism as boron reacts here like a typical radical, e.g., a halogen atom.[52] The $2p_x$, $2p_y$, and $2p_z$ AOs of boron transform according to a′, a″, and a′, respectively (Figure 5) giving rise to three states, ^{2}A′, ^{2}A″, and ^{2}A′. These states are degenerate at large benzene−boron separations. As the ^{2}A′ state of **4**-C_s correlates with the ground states of the reactants, formation of **4** is not hampered by orbital symmetry imposed barriers.

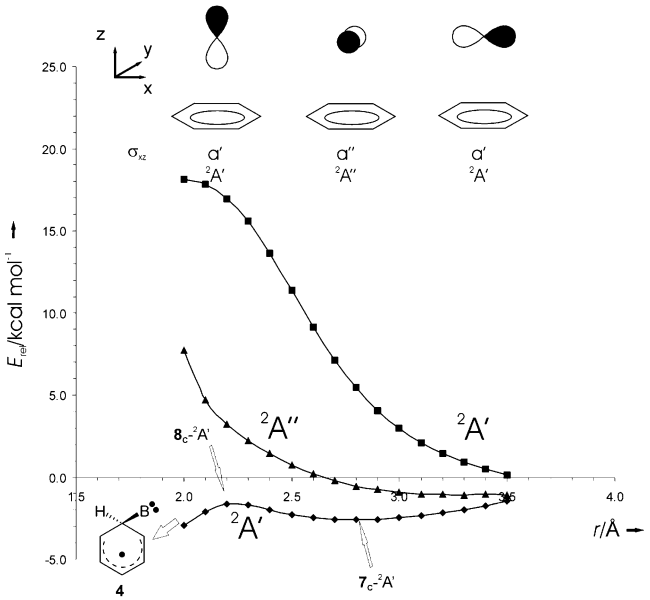

Figure 5. Attack of boron atom in C_s symmetry at a corner of benzene. The potential energy curves of the three lowest energy states were computed at the state averaged MC-QDPT2/cc-pVTZ//(9,10)-CASSCF/6-31G* level of theory.

TABLE 1: Reaction Energies (in kcal mol^{-1}) for Formation of C_6H_5B Isomers and C_6H_5 + BH from C_6H_6 + B(^{2}P) As Computed at Various Levels of Theory Including Zero-Point Vibrational Energy Corrections

species	state	B3LYP/6-311+G**	CCSD(T)/cc-pVTZ[a]
1 + H	$^1A_1$ + ^2S	−23.0	−19.2
[D_5]-**1** + D	$^1A_1$ + ^2S	−20.5	−16.7
2 + H	$^1A_1$ + ^2S	12.8	12.7
[D_5]-**2** + D	$^1A_1$ + ^2S	14.8	14.7
3 + H	^1A + ^2S	16.5	23.3
[D_5]-**3** + D	^1A + ^2S	18.6	25.4
9 + BH	$^2A_1$ + $^1\Sigma^+$	28.9	30.4
[D_5]-**9** + BD	$^2A_1$ + $^1\Sigma^+$	30.1	31.6

[a] Using the B3LYP/6-311+G** geometries and ZPVE corrections.

The description of the ^{2}A′ entrance channel by B3LYP is anticipated to be difficult due to dispersion interactions as well as the near degeneracy of the ^{2}A′ states at large benzene−boron separations. Hence, potential energy curves (Figure 5) were computed at the (9,10)-CASSCF/6-31G* level of theory by constraining the C−B distance and optimizing all other degrees of freedom within C_s symmetry. The geometries thus obtained were used in state-averaged MC-QDPT2/cc-pVTZ single point computations for refinement of energies. The π complex on the ^{2}A′ ground state potential energy curve (**7$_C$**-^{2}A′) obtained from the MC-QDPT2 computations is characterized by a benzene−boron separation of approximately 2.8 Å and an energy of −2.6 kcal mol^{-1}. This is in good agreement with the CCSD(T)//B3LYP result: **7$_C$**-^{2}A′ has a large C−B distance of 2.79 Å after full geometry optimization (B3LYP/6-311+G**) and lies 2.6 kcal mol^{-1} (1.3 kcal mol^{-1} at B3LYP) (Table 2) below reactants. With decreasing C−B distance, the energy increases and the system has to go over a small barrier (**8$_C$**-^{2}A′) of about 1 kcal mol^{-1} (MC-QDPT2/cc-pVTZ//(9,10)-CASSCF/6-31G*) before formation of the first addition product **4** is complete. In contrast, the ^{2}A″ and excited ^{2}A′ state PESs are repulsive over the entire r(C−B) range at the MC-QDPT2/cc-pVTZ//(9,10)-CASSCF/6-31G* level of theory. Finally, note that the product (**4**) of addition to the benzene corner and the long-range π complex **7$_C$**-^{2}A′ are related to the π and σ complexes that halogen atoms form with benzene, as studied recently by Tsao et al.[52]

TABLE 2: Energies (in kcal mol^{-1}) of C_6H_6B Species Relative to the Most Stable One, C_6H_5–BH (10), As Computed at Various Levels of Theory Including Zero-Point Vibrational Energy Corrections

species	state	B3LYP/6-311+G** [a]	CCSD(T)/cc-pVTZ[b]
C_6H_6 + B	$^1A_{1g}$ + ^2P	66.4	61.2
4-C_s	^{2}A′	57.0 (1)	52.7
4-C_1	^{2}A	57.1	52.9
5	^{2}A″	57.9 (1)	53.2
6	^{2}A′	35.3	24.7
6-C_{2v}	^{2}A′	41.7	32.5
7$_C$-^{2}A′	^{2}A′	65.2	58.6
7$_E$-^{2}A′	^{2}A′	65.2	58.6
7$_E$-^{2}A″	^{2}A″	65.7	59.4
8$_E$-^{2}A′	^{2}A′	68.0 (2)	
8$_E$-^{2}A″	^{2}A″	65.7 (1)	60.3
10 (planar-bent)	^{2}A′	0	0
10 (bisected)	^{2}A′	1.5 (1)	3.1
10-C_{2v}	$^2B_1$	3.5 (1)	6.7
10-C_{2v}	$^2B_2$	8.9 (1)	10.7
11	$^2A_1$	9.9	12.0
12	^{2}A	47.7	
13	^{2}A′	8.2	11.6
14	^{2}A	38.6	29.8
TS1	^{2}A′	61.7 (1)	60.1
TS2	^{2}A	58.4 (1)	54.8
TS3	^{2}A	47.4 (1)	
TS4	^{2}A	52.3 (1)	57.3
TS5	^{2}A	26.2 (1)	29.4
TS6	^{2}A	95.5 (1)	88.8
TS7	^{2}A	51.7 (1)	47.3
TS8	^{2}A	50.5 (1)	44.8
TS9	^{2}A	47.7 (1)	48.9
[D_6]-**TS9**	^{2}A	49.9 (1)	51.1

[a] The number of imaginary vibrational frequencies is given in parentheses. [b] Using the B3LYP/6-311+G** geometries and ZPVE corrections.

We next consider attack of the boron atom at an *edge* of benzene. The $2p_x$, $2p_y$, and $2p_z$ AOs transform now according to a″, a′, and a′, respectively (Figure 6). As above, the resulting states need to be degenerate at very large C−B distances.

Let us first consider the ^{2}A″ PES, which we have investigated with the B3LYP/6-311+G** method (Figure 6). Edge-bridged **5** correlates with a π complex (**7$_E$**-^{2}A″, −1.8 kcal mol^{-1}), which is a minimum at the B3LYP level. Upon further approach of boron to benzene, the ^{2}A″ PES is slightly repulsive and a barrier of 0.4 kcal mol^{-1} (without ZPVE correction) through transition state **8$_E$**-^{2}A″ (152i cm^{-1}, a′) has to be passed before the energy of the system decreases. The IRC (displayed in Figure 6) connects transition state **8$_E$**-^{2}A″ to **7$_E$**-^{2}A″ on one side and to **5** on the other side of the potential. However, as **5** has an imaginary vibrational frequency of a″ symmetry, there must be a valley ridge inflection (VRI) point[53−55] somewhere along the path between **8$_E$**-^{2}A″ and **5**. By computing the projected Hessian matrix for points along the IRC, we have narrowed the VRI region to the vicinity of structures with C1−B distances of 2.93 Å, 2.8−2.9 kcal mol^{-1} (B3LYP/6-311+G**) below transition state **8$_E$**-^{2}A″. The IRC no longer follows a valley beyond the VRI point, but rather descends on a ridge to **5**. The real reacting system possessing kinetic energy can deviate from the IRC to ultimately end at the addition product **4**.[56]

The situation becomes more complex when the ^{2}A′ state surface is considered in addition. At short benzene−boron separations, the 7-boranorbornadiene-7-yl radical (**6**, ^{2}A′) is much lower in energy (by 28.4 kcal mol^{-1}) than the formal addition product **5** on the ^{2}A″ PES. The ^{2}A′ potential energy curve connects **6** to the separated products; however, this

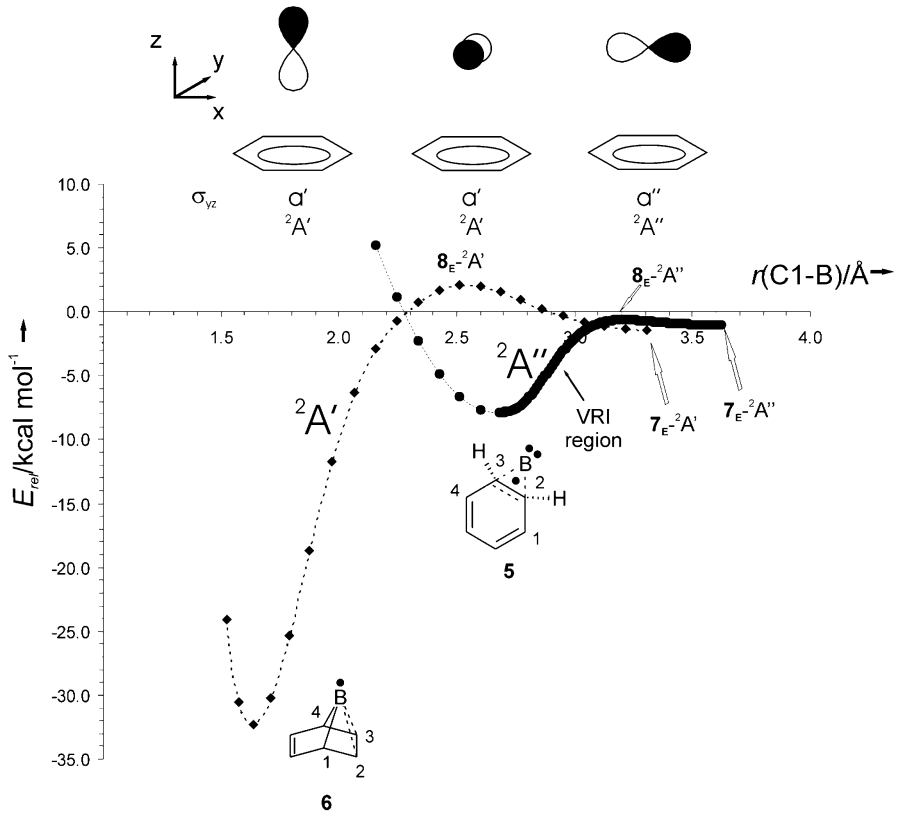

Figure 6. Attack of boron atom in C_s symmetry at an edge of benzene. The potential energy curves were obtained at the B3LYP/6-311+G** level of theory by either an IRC computation (^{2}A″, thick solid line) or geometry optimizations with fixed C1−B distances (^{2}A′ and ^{2}A″, dotted and broken lines).

potential energy curve does not follow a valley at large benzene−boron separations, but rather runs on a ridge: the π complex **7**$_E$-^{2}A′ has an imaginary vibrational frequency of 53i cm^{-1} (a″ symmetry) at B3LYP/6-311+G**.[57] Similarly, the maximum of the ^{2}A′ curve (**8**$_E$-^{2}A′) in Figure 6 does not correspond to a transition state, but rather to a second-order stationary point (247i cm^{-1}, a′; and 190i cm^{-1}, a″). Although the C1−B distance is shorter by 0.22 Å in the (9,10)-CASSCF/6-31G* geometry of **8**$_E$-^{2}A′, qualitative agreement with the B3YLP/6-311+G** result is obtained. In particular, **8**$_E$-^{2}A′ is also a second-order stationary point at (9,10)-CASSCF/6-31G* (357i cm^{-1}, a′; and 182i cm^{-1}, a″). The path of boron to the benzene edge within ^{2}A′ state symmetry runs on the ridge between two symmetry equivalent reaction valleys of corner attack. Hence, attack of boron at the benzene edge is unfavorable on the ^{2}A′ PES: the system breaks symmetry and attacks the corner of benzene on the ^{2}A′ PES resulting in **4**.

However, the ^{2}A′ potential energy curve crosses the ^{2}A″ curve twice: at short C1−B (∼2.3 Å) and long C1−B (∼3.1 Å) distances. A similar crossing of surfaces in the entrance channel has been recognized by Flores and Largo for the reaction of B atom with acetylene,[8] and later also invoked by Balucani et al.[12,14] A consequence of these crossings of states is the possibility of nonadiabatic transitions from one surface to the other; formation of **6** directly from benzene and boron might thus be possible. In our case, however, there is one important issue, which renders this event unlikely: at the short distance crossing, the ^{2}A″ curve no longer runs on the floor of a valley, but rather on a ridge. Hence, the reacting system following the ^{2}A″ state could have relaxed to **4** before it has a chance to come close to the short distance state crossing.[58]

We finally consider the addition of boron to benzene in C_{2v} symmetry on the ^{2}A$_1$ surface to yield **6**-C_{2v}, formally a least motion [4 + 2] cycloaddition. A maximum along this path (**8**$_{C_{2v}}$-^{2}A$_1$) lies 9 kcal mol^{-1} (MC-QDPT2/cc-pVTZ//(9,10)-CASSCF/6-31G*) higher in energy than separated reactants, but it is a third-order stationary point with b_1, b_2, and a_1 imaginary vibrational frequencies. The b_1 mode corresponds to tilting of the developing boron atom bridge as described for **6**-C_{2v} above. Relaxation from C_{2v} into C_s symmetry according to this mode turns the ^{2}A$_1$ and ^{2}B$_1$ states, which are essentially isoenergetic at the **8**$_{C_{2v}}$-^{2}A$_1$ geometry, into two ^{2}A′ states. These states split due to strong interaction. On the lower energy ^{2}A′ surface the relaxation of geometry should result in **8**$_E$-^{2}A′, which is a second-order stationary point as discussed above.

In summary, we could not find a direct low-energy pathway for the benzene + B(^{2}P) reactants to form the very stable **6**. This is in contrast to the valence-isoelectronic Al−benzene system, for which matrix isolation ESR experiments[24,25] were interpreted[25] in terms of a transannular addition product analogous to **6**. As the experiments studied the co-condensation of benzene and aluminum evaporated from an ∼1000 °C furnance, a higher energy reaction path might be accessible under such conditions. A computational investigation of the entrance channels similar to the one above is not available, but would be necessary for a detailed comparison of the boron and aluminum reactions with benzene.

Abstraction of Benzene Hydrogen by Boron. The abstraction of a hydrogen from benzene by a boron atom yields phenyl radical (**9**) and BH($^1\Sigma^+$). The reaction, however, is strongly endoergic (ΔH(0 K) = +30.4 kcal mol^{-1}). For the perdeuterated system yielding [D$_5$]-phenyl radical and BD, this value is +31.6 kcal mol^{-1} (Table 1). The abstraction reaction is therefore not important under the low collision energy (5.5 kcal mol^{-1}) conditions of our experiment. We therefore do not consider this reaction further in this work.

SCHEME 2: Rearrangements from Primary Boron Addition Products 4 and 6 to Benzoborirene (1) and Hydrogen Atom Involving a Number of Minima and Transition States

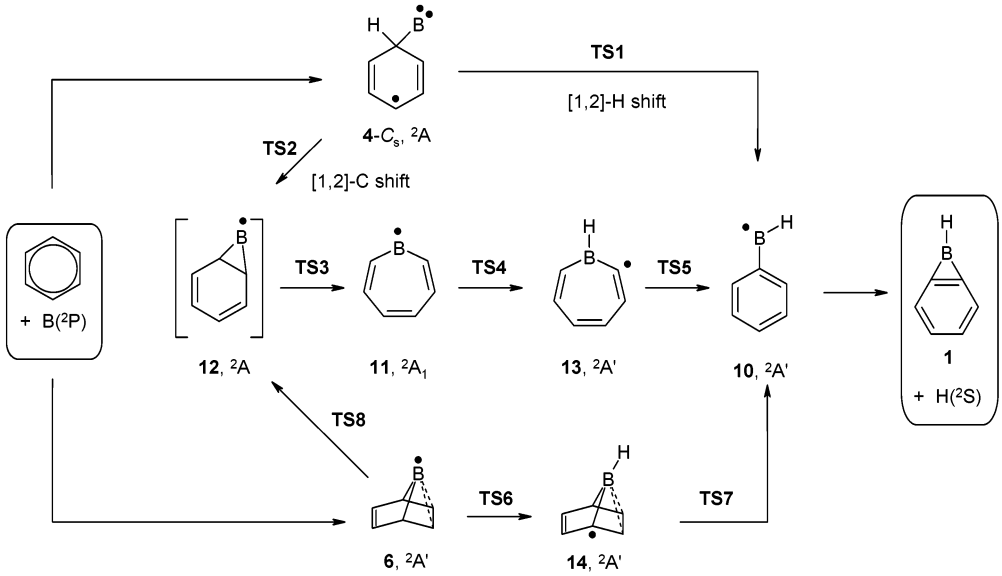

B. Rearrangements on the C_6H_6B Potential Energy Surface. Having identified **4** (and with a lower probability **6**) as the important product of addition of boron to benzene, we now investigate intramolecular rearrangements on the way to **1** + H. Two pathways are conceivable for **4**: (i) [1,2]-H shift to yield phenylboryl radical (**10**) and (ii) [1,2]-C shift to yield the borepinyl radical (**11**) (Scheme 2). The transition state **TS1** (Figure 2) for the [1,2]-H shift is of C_s symmetry (^{2}A′). The boron atom is tilted considerably toward the benzene ring plane, while the migrating hydrogen is bridging the C−B bond. The barrier for the very exoergic (−53 kcal mol^{-1}) hydrogen shift is found to be 7.5 kcal mol^{-1}. This value is about 3 kcal mol^{-1} larger than the MC-QDPT2/cc-pVTZ//(9,10)-CASSCF/6-31G*+ZPVE and B3LYP/6-311+G**+ZPVE barriers, which are both 4.7 kcal mol^{-1}.

The product of [1,2]-H shift, phenylboryl radical (**10**), has previously been investigated computationally by Rablen and Hartwig at the CBS-4 level of theory.[59] In agreement with these authors, we find that **10** prefers a planar structure (^{2}A′) with a bent geometry at boron, ∠(C−B−H) = 128.2°. Compared to the reactants, **10** is very low in energy (−61.2 kcal mol^{-1}), making it the most stable C_6H_6B species considered in this study. We also considered other geometries and electronic states of **10**. If the single electron is moved from the sp^2-type SOMO into a π(B) MO, the resulting ^{2}A″ state adopts a linear C−B−H geometry; this state is ^{2}B$_1$ in terms of C_{2v} symmetry. Besides the ^{2}B$_1$, a ^{2}B$_2$ state is also possible for the C_{2v} structure of **10** (Figure 7). While both states correspond to first-order stationary points, the ^{2}B$_1$ state (6.8 kcal mol^{-1} with respect to **10**) is more favorable than the ^{2}B$_2$ state (10.6 kcal mol^{-1}). In addition, bisected geometries are conceivable for **10**, and again two states, ^{2}A′ and ^{2}A″, need to be considered. The ^{2}A′ state is a transition state, 3.1 kcal mol^{-1} higher in energy than **10**. This corresponds to the barrier for rotation of the BH unit around the C−B single bond. The ^{2}A″ state, on the other hand, avoids the bisected geometry by converging to the linear C−B−H moiety of ^{2}B$_2$-**10**.

The barrier for ring enlargement of **4** to **11** through **TS2** is only 2 kcal mol^{-1}. An asymmetric bicyclic structure **12** with a very long C−C bond (1.710 Å) bridged by boron corresponds to a very shallow minimum on the **4** → **11** pathway: the classical barrier for the strongly exoergic (−37.7 kcal mol^{-1} at B3LYP/6-311+G**) ring opening to borepinyl radical **11** is less than 0.01 kcal mol^{-1} through **TS3**. After inclusion of ZPVE corrections, the **TS3** (128i cm^{-1}, r(C−C) = 1.750 Å) lies even lower in energy than **12** by 0.2 kcal mol^{-1} (B3LYP/6-311+G**). As **12** is rather unimportant in the overall reaction mechanism, we have made no attempts to study it at more sophisticated computational levels.

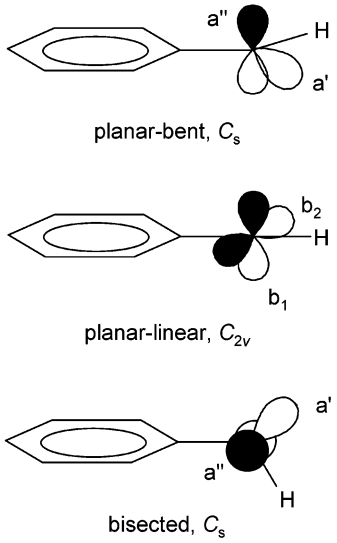

Figure 7. Molecular orbitals and their symmetries in the three conformations of phenylboryl radical (**10**).

The boron-centered radical **11** is less stable than its isomer **13** by 0.4 kcal mol^{-1}. The **TS4** interconnecting **11** and **13** lies high in energy (45.2 kcal mol^{-1} with respect to **11**). It is nonplanar as the carbon and boron atoms involved in the hydrogen shift are moved away from the ring plane (Figure 2). While the C−H distance is increased to 1.451 Å, the B−H distance is 1.357 Å. The seven-membered-ring system **13** can contract to **10**, thereby gaining 11.6 kcal mol^{-1}. This rearrangement requires a barrier (via **TS5**) of 17.7 kcal mol^{-1} to be overcome. The newly forming C−C bond is well developed in **TS5** as the CC distance is 1.875 Å compared to 2.589 Å in **13**.

The phenylboryl and borepinyl radicals **10** and **11** are also accessible from the addition product **6**. A hydrogen shift yields

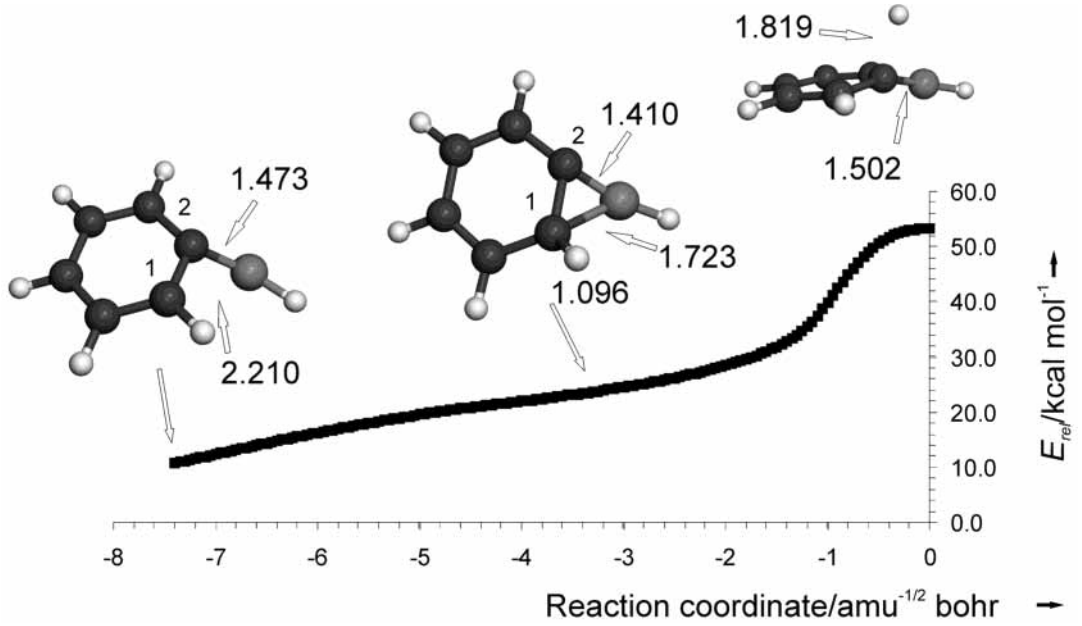

Figure 8. Plot of energy (relative to phenylboryl radical **10**) versus intrinsic reaction coordinate (IRC) for attack of a hydrogen atom on benzoborirene (**1**) starting at the transition state (**TS9**). While **TS9** is close to **1** in geometry, the last point along the IRC is close to **10**. Carbon, dark gray; boron, light gray; hydrogen, small balls.

14 from **6**, but the barrier through **TS6** is very high, 64.0 kcal mol^{-1}. The product **14** of this [1,2]-H shift to boron is only 5.1 kcal mol^{-1} less stable than **6**. Subsequent C−B bond breaking in **14** via **TS7** and rearrangement to **10** involves a barrier of only 17.4 kcal mol^{-1}. The energetically more favorable reaction channel starting at **6** is the rearrangement to **11**, which has a barrier through **TS8** of only 20.0 kcal mol^{-1}. The bridgehead C4−B bond is strongly elongated (2.454 Å), while the C2−B distance is shortened to 1.547 Å. The C1−C2 bond, which ultimately needs to break for formation of **11**, is stretched only somewhat, to 1.590 Å, in **TS8**. Indeed, **12** is a formal intermediate in this rearrangement, but as discussed above, **12** disappears after inclusion of ZPVE corrections.

C. Exit Channels. We have investigated the loss of a hydrogen atom from the energetically low lying C_6H_6B species **10**, and the borepinyl isomers **11** and **13** resulting in **2** and **3**, respectively. However, no transition states for these reactions could be located. Hence, these C_6H_6B isomers can form phenylborylene (**2**) + H and didehydroborepine (**3**) + H without barriers on the potential energy surfaces. Alternatively, the C_6H_5B species **2** and **3** can react with hydrogen atoms without the involvement of any barriers. These isomers, however, are high in energy compared to **1** (see Table 1), and hence the latter is observed.

We could locate a transition state **TS9** for formation of **1** + H from **10**. In agreement with the Hammond postulate, the transition state is late on the reaction coordinate and resembles the benzoborirene (**1**) product. For convenience we consider now the reverse reaction, i.e., the attack of a hydrogen atom on one of the two bridgehead carbon atoms of **1**. The barrier for this addition reaction is 6.9 kcal mol^{-1} (4.3 kcal mol^{-1} at B3LYP). As the C−H distance in **TS9** is as large as 1.819 Å, the pyramidalization of the bridgehead carbon atom is small. The sum of covalent angles (i.e., ignoring the attacking H atom) around this bridgehead carbon atom is 349.5° rather than 360° in **1**. This angle sum is 356.2° at the bridgehead atom not attacked by H. The C(H)−B distance is somewhat longer (1.502 Å) than in **1** (1.480 Å), while the other C−B bond (1.467 Å) is slightly shortened. The angles involving the forming C−H bond are 114.9° to the other bridgehead carbon, 99.0° to the ortho carbon atom, and 90.1° to boron. A qualitatively similar geometry was also obtained at the (7,8)-CASSCF/6-31G* level of theory. Here, however, the C−H distance is much shorter, 1.652 Å, and consequently the pyramidalization is more pronounced as the angle sums are 339.0° and 352.4°. Using the H−C(bridge)−C(bridge) angle as an indicator for the orientation of the attacking hydrogen atom to the six-membered ring, we conclude that the attack is closer to being orthogonal to the six-membered ring at the CASSCF (109.9°) level than at B3LYP (114.9°). In agreement with the much tighter geometry of the transition state at the CASSCF level, the imaginary vibrational frequency is significantly larger (1322i cm^{-1}) than at B3LYP (757i cm^{-1}). Although CASSCF often gives a qualitatively correct surface, it is well-known that extensive dynamic correlation is required to achieve quantitative results.[60] This is very likely also the case for the present transition state.

The expected product of the addition of an H atom to **1**, the bicyclic bridgehead radical does not correspond to a stationary point at B3LYP or (7,8)-CASSCF levels. Rather, the ring-opened phenylboryl radical **10** resulted. This is also supported

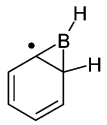

by IRC computations (Figure 8). After a steep descent from **TS9**, the reaction coordinate passes through a rather flat part of the PES. The geometries resemble the bicyclic bridgehead radical in this area, but the IRC does not stop here. The last point we computed on the IRC is characterized by a long C1−B distance of 2.210 Å, while the C2−B bond is 1.473 Å, already close to the 1.527 Å in **10**. Clearly, the addition reaction of a hydrogen atom to benzoborirene results directly in the phenylboryl radical **10**. Conversely, the formation of **1** + H must start from **10** and proceed over a rather large barrier of 48.9 kcal mol^{-1} (47.7 kcal mol^{-1} at B3LYP).

D. Potential Energy Surface of C_6H_6 + B Reaction: The Most Favorable Reaction Path. We are now in a position to elucidate the energetically most favorable reaction path from

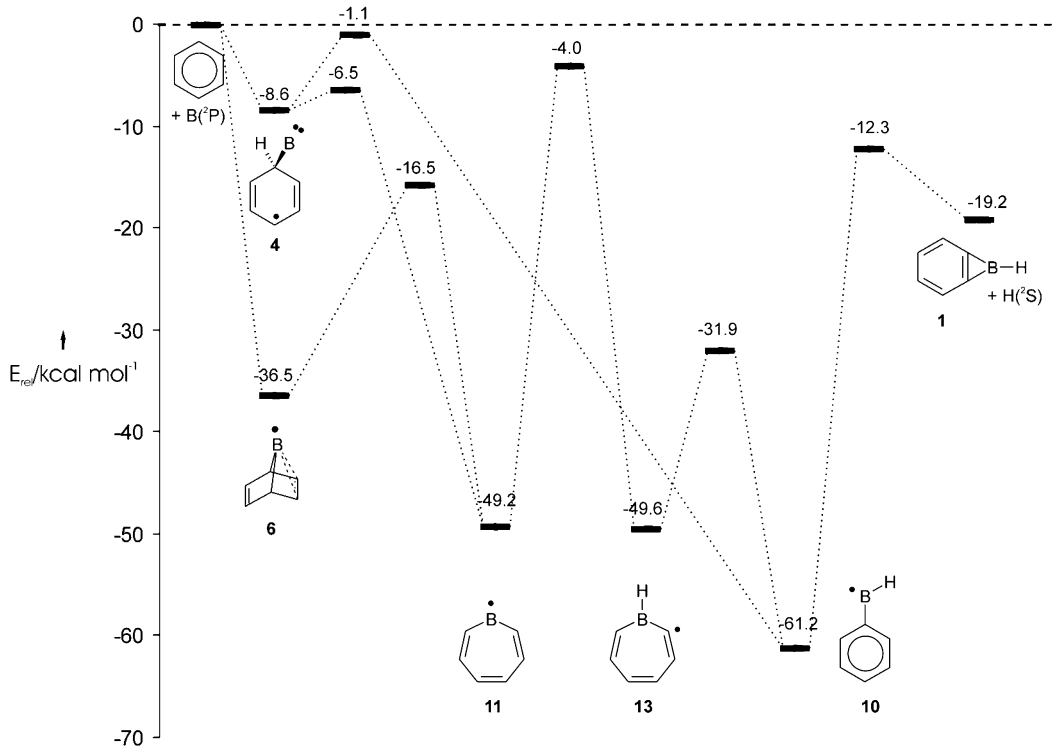

Figure 9. Schematic representation of potential energy surface for formation of benzoborirene (**1**) + H(^{2}S) from benzene and B(^{2}P). All energies given were obtained at the CCSD(T)/cc-pVTZ//B3LYP/6-311+G** + ZPVE(B3LYP/6-311+G**) level of theory. Endoergic reaction paths (with respect to reactants) are not depicted.

reactants, C_6H_6 + B(^{2}P), to products, **1** + H. Consequently, all energies here are given relative to separated reactants.

The attack of the benzene π system by the boron atom at the corner (^{2}A′) or at the edge (^{2}A″) of the benzene hexagon yields **4** in both cases (a VRI point is involved in the latter case). Prereactive π complexes precede the formation of **4** (not depicted in Figure 9), but the barriers in both of these entrance channels are below the energy of the reactants. Consequently, the initial product **4** can be formed without additional energy.

Formation of **6** by attack at the benzene edge requires a nonadiabatic transition from the ^{2}A″ to the ^{2}A′ PES in the vicinity of an intersection of these states. However, as detailed in section A, the reacting system is unlikely to come close to this crossing of states.

Irrespective of the details of the entrance channels, the primary addition products **4** or **6** rearrange preferably to **11**, the product of overall CC insertion. Formation of the CH-insertion product **10** is less favorable from **4** and not possible from **6** under our experimental conditions (vide infra) due to an extremely high barrier (+27.5 kcal mol^{-1} with respect to reactants). The CH-insertion product **10** is nonetheless of crucial importance as it provides the C_6H_6B system, which has accumulated more than 60 kcal mol^{-1} by now, with a low-energy exit pathway to **1** + H. The **11** → **13** → **10** rearrangements have energy requirements below the energy of reactants and thus offer a viable link between CC- and CH-insertion products.

A comparison of the energies computed with B3LYP and CCSD(T)//B3LYP is appropriate (Table 2). Taking the latter level of theory as a reference, we find that B3LYP overestimates the stability of the bora-aromatic species **1** and **3** by approximately 4 and 7 kcal mol^{-1} (Table 1), respectively. The boranorbornadienyl species **6**, **6**-C_{2v}, **14**, and **TS6**, however, are exceptional: B3LYP places them up to 11 kcal mol^{-1} higher in energy than CCSD(T). Nonetheless, the B3LYP and CCSD(T) surfaces agree qualitatively and the differences in energies are not critical to the basic conclusions of this work. In particular, the barrier for formation of **1** + H from **10** is very similar at the B3LYP and CCSD(T) levels.

E. Comparison with Experimental Results. Information on the product isomer and on the underlying reaction mechanism can be obtained by analyzing the center-of-mass functions. First, the maximum translation energy E_{max} of $P(E_T)$ of 19−21.5 kcal mol^{-1} could be utilized to identify the nature of the product isomer. Basically, E_{max} is the sum of the reaction exoergicity plus the collision energy. Subtracting the collision energy from E_{max}, the exoergicity of the reaction of atomic boron with [D_6]-benzene is calculated to be 14.8 ± 1.2 kcal mol^{-1}. Comparison of the computed energy balance for formation of feasible reaction products ([D_5]-**1**, [D_5]-**2**, and [D_5]-**3**) and deuterium atom allows assignment of the observed $^{11}BC_6D_5$ product. An agreement between experimental and theoretical reaction energies is reached for formation of [D_5]-**1** + D from the reactants, while the reactions yielding [D_5]-**2** + D or [D_5]-**3** + D are endoergic by +14.7 kcal mol^{-1} and +25.4 kcal mol^{-1}, respectively. Neither of these isomers can be formed since the collision energy in our experiments was only 5.5 kcal mol^{-1}.

These combined experimental and theoretical investigations do not only identify the reaction products unambiguously, but ascertain also the reaction mechanism. The angular flux distribution depicts a symmetric profile around 90°;[16] this shape characterizes a bimolecular reaction which goes though an intermediate $^{11}BC_6D_6$ having a lifetime larger than its rotation period. The peaking at 90° suggests further that the deuterium atom is ejected perpendicular to the molecular plane of the $^{11}BC_6D_5$ moiety. Here, the shape of the $T(\theta)$ is determined by the disposal of the total angular momentum **J**. In our crossed-beam experiment, the benzene molecular beam undergoes a supersonic expansion and a substantial rotational cooling of benzene molecules occurs. Hence the total angular momentum

is mainly given by the initial orbital angular momentum **L**. The products can be rotationally excited, however, so that eq 1 is valid:

$$\mathbf{J} \approx \mathbf{L} \approx \mathbf{L}' + \mathbf{j}' \quad (1)$$

with the rotational angular momenta of the products **j′**, and the initial and final orbital angular momenta **L** and **L′**. The final recoil velocity vector, **v′**, is in a plane perpendicular to **L′**, and therefore, when the rotational excitation of products is important, **v′** is not in a plane perpendicular to **J**. When **j′** is not zero, the probability distribution for the scattering angle θ, which is the center-of-mass angle between the initial relative velocity **v** and **v′**, depends on the values of J, M, and M', where M and M' are the projections of **J** on the initial velocity and final relative velocity, respectively. If the complex dissociates preferentially with low M' values, the final velocity **v′** is almost perpendicular to **J** and therefore **v′** and **v** are almost parallel. In this case, the product intensity will be mainly confined to the poles, $\theta = 0°$ and $\theta = 180°$, similar to the case of no product rotational excitation. On the other hand, when the collision complex dissociates mainly with high M' values, the final relative velocity will be almost parallel to **J** and perpendicular to **v** and the products will be preferentially scattered at $\theta = 90°$ as observed in our experiment. Considering the reverse reaction, the deuterium atom then attacks perpendicular to the molecular plane of benzoborirene. Similar to the addition of a hydrogen atom to the aromatic benzene molecule,[61] this process is expected to have an entrance barrier. The existence of an entrance barrier for the reversed reaction, i.e., the addition of the deuterium atom to the benzoborirene molecule, is well reflected in the distribution maximum of the center-of-mass translational energy distribution, $P_{max}(E)$, of 2.4−4.8 kcal mol^{-1}. These data give the order of magnitude of the barrier height in the exit channel and suggest a significant geometry as well as electron density change from the decomposing $^{11}BC_6D_6$ intermediate to the products. These findings are supported by our electronic structure computations. We find a barrier for addition of a deuterium atom to one of the bridgehead carbon atoms in **1** of 4−7 kcal mol^{-1}. Likewise, the attacking deuterium atom is oriented almost perpendicularly to the molecular plane of **1** in the transition state.

Conclusions

From our combined experimental and computational investigation of the $C_6D_6 + B(^2P)$ reaction we conclude the following:

(1) Under the single-collision, low collision energy conditions of the crossed-beam experiment, the reaction yields the benzoborirene molecule and a deuterium atom. This conclusion is based on the agreement between experimental and computational reaction exoergicity, transition state structure, and barrier height in the exit channel, and is in agreement with the results reported in our preliminary communication.[16]

(2) There are two modes of addition of boron to the π system of benzene: addition to the corner and to the edge of a benzene hexagon. Neither involves barriers higher in energy than benzene + B. Benzene and boron atom can form a π complex (**7$_C$**-^{2}A′) and a σ complex (**4**). In both of these complexes boron has η_1 coordination. The σ complex is more stable than the π complex by 6.0 kcal mol^{-1} at the CCSD(T)/cc-pVTZ//B3LYP/6-311+G** + ZPVE level of theory. The second channel, addition to the edge of a benzene hexagon, following the ^{2}A″ state ultimately results in **4** due to a valley ridge inflection (VRI) point. Another consequence of this VRI point on the ^{2}A″ PES is that the reacting system is unlikely to reach a crossing with the ^{2}A′ state, where a nonadiabatic transition could lead to the 7-boranorbornadiene-7-yl radical (**6**, ^{2}A′).

(3) Abstraction of hydrogen from benzene by boron atom is too endoergic to be of importance in our experiment.

(4) Rearrangements of **4** and **6** ultimately lead to phenylboryl radical (**10**) and do not involve barriers higher than the energy of the reactants.

(5) Phenylboryl radical (**10**) can react to benzoborirene (**1**) and hydrogen by cleavage of an ortho-CH bond and concomitant closure of the C−B bond.

Acknowledgment. H.F.B. thanks the Fonds der Chemischen Industrie for continued support through a Liebig Fellowship and Professor Dr. W. Sander for encouragement.

References and Notes

(1) Jeong, G.; Klabunde, K. J. *J. Am. Chem. Soc.* **1986**, *108*, 7103.
(2) Lebrilla, C. B.; Maier, W. F. *Chem. Phys. Lett.* **1984**, *105*, 183.
(3) Hassanzadeh, P.; Andrews, L. *J. Am. Chem. Soc.* **1992**, *114*, 9239.
(4) Hassanzadeh, P.; Hannachi, Y.; Andrews, L. *J. Phys. Chem.* **1993**, *97*, 6418.
(5) Hannachi, Y.; Hassanzadeh, P.; Andrews, L. *J. Phys. Chem.* **1994**, *98*, 6950.
(6) Martin, J. M. L.; Taylor, P. R.; Hassanzadeh, P.; Andrews, L. *J. Am. Chem. Soc.* **1993**, *115*, 2510.
(7) Andrews, L.; Hassanzadeh, P.; Martin, J. M. L.; Taylor, P. R. *J. Phys. Chem.* **1993**, *97*, 5839.
(8) Flores, J. R.; Largo, A. *J. Phys. Chem.* **1992**, *96*, 3015.
(9) Andrews, L.; Lanzisera, D. V.; Hassanzadeh, P.; Hannachi, Y. *J. Phys. Chem. A* **1998**, *102*, 3259.
(10) Lanzisera, D. V.; Andrews, L. *J. Phys. Chem. A* **1997**, *101*, 1482.
(11) So, S. P. *J. Phys. Chem. A* **2002**, *106*, 3181.
(12) Balucani, N.; Asvany, O.; Lee, Y. T.; Kaiser, R. I.; Galland, N.; Hannachi, Y. *J. Am. Chem. Soc.* **2000**, *122*, 11234.
(13) Galland, N.; Hannachi, Y.; Lanzisera, D. V.; Andrews, L. *Chem. Phys.* **1998**, *230*, 143.
(14) Balucani, N.; Asvany, O.; Lee, Y. T.; Kaiser, R. I.; Galland, N.; Rayez, M. T.; Hannachi, Y. *J. Comput. Chem.* **2001**, *22*, 1359.
(15) Sillars, D.; Kaiser, R. I.; Galland, N.; Hannachi, Y. *J. Phys. Chem. A* **2003**, *107*, 5149.
(16) Kaiser, R. I.; Bettinger, H. F. *Angew. Chem.* **2002**, *114*, 2456; *Angew. Chem., Int. Ed.* **2002**, *41*, 2350.
(17) Eckert-Maksic, M.; Glasovac, Z.; Maksic, Z. B.; Zrinski, I. *THEOCHEM* **1996**, *366*, 173.
(18) Stanger, A. *J. Am. Chem. Soc.* **1998**, *120*, 12034.
(19) Maksic, Z. B.; Eckert-Maksic, M.; Pfeifer, K.-H. *J. Mol. Struct.* **1993**, *300*, 445.
(20) Fox, W. B.; Ehrlich, R.; Pez, G. *Preparation, properties, and reactions of reactive inorganic intermediates in the formation of new materials*; Deparment of the Air Force, Air Force Office of Scientific Research: Washington, DC, 1970.
(21) Ramsey, B. G.; Anjo, D. M. *J. Am. Chem. Soc.* **1977**, *99*, 3182.
(22) Calhoun, G. C.; Schuster, G. B. *J. Org. Chem.* **1984**, *49*, 1925.
(23) Uddin, J.; Boehme, C.; Frenking, G. *Organometallics* **2000**, *19*, 571.
(24) Kasai, P. H.; McLeod, D. *J. Am. Chem. Soc.* **1979**, *101*, 5860.
(25) Howard, J. A.; Joly, H. A.; Mile, B. *J. Am. Chem. Soc.* **1989**, *111*, 8094.
(26) Mitchell, S. A.; Simard, B.; Rayner, D. M.; Hackett, P. A. *J. Phys. Chem.* **1988**, *92*, 1655.
(27) McKee, M. L. *J. Phys. Chem.* **1991**, *95*, 7247.
(28) Silva, S. J.; Head, J. D. *J. Am. Chem. Soc.* **1992**, *114*, 6479.
(29) Becke, A. D. *J. Chem. Phys.* **1993**, *98*, 5648.
(30) Stephens, P. J.; Devlin, F. J.; Chabalowski, C. F.; Frisch, M. J. *J. Phys. Chem.* **1994**, *98*, 11623.
(31) Frisch, M. J.; Trucks, G. W.; Schlegel, H. B.; Scuseria, G. E.; Robb, M. A.; Cheeseman, J. R.; Zakrzewski, V. G.; Montgomery, J. A., Jr.; Stratmann, R. E.; Burant, J. C.; Dapprich, S.; Millam, J. M.; Daniels, A. D.; Kudin, K. N.; Strain, M. C.; Farkas, O.; Tomasi, J.; Barone, V.; Cossi, M.; Cammi, R.; Mennucci, B.; Pomelli, C.; Adamo, C.; Clifford, S.; Ochterski, J.; Petersson, G. A.; Ayala, P. Y.; Cui, Q.; Morokuma, K.; Salvador, P.; Dannenberg, J. J.; Malick, D. K.; Rabuck, A. D.; Raghavachari, K.; Foresman, J. B.; Cioslowski, J.; Ortiz, J. V.; Baboul, A. G.; Stefanov, B. B.; Liu, G.; Liashenko, A.; Piskorz, P.; Komaromi, I.; Gomperts, R.; Martin, R. L.; Fox, D. J.; Keith, T.; Al-Laham, M. A.; Peng, C. Y.; Nanayakkara, A.; Challacombe, M.; Gill, P. M. W.; Johnson, B.; Chen,

W.; Wong, M. W.; Andres, J. L.; Gonzalez, C.; Head-Gordon, M.; Replogle, E. S.; Pople, J. A. *Gaussian 98*, Revision A.11; Gaussian, Inc.: Pittsburgh, PA, 2001.

(32) Lee, C.; Yang, W.; Parr, R. G. *Phys. Rev. B* **1988**, *37*, 785.

(33) Gonzalez, C.; Schlegel, H. B. *J. Chem. Phys.* **1989**, *90*, 2154.

(34) Gonzalez, C.; Schlegel, H. B. *J. Phys. Chem.* **1990**, *94*, 5523.

(35) Raghavachari, K.; Trucks, G. W.; Pople, J. A.; Head-Gordon, M. *Chem. Phys. Lett.* **1989**, *157*, 479.

(36) Hampel, C.; Peterson, K.; Werner, H.-J. *Chem. Phys. Lett.* **1992**, *190*, 1.

(37) Dunning, T. H. *J. Chem. Phys.* **1989**, *90*, 1007.

(38) Knowles, P. J.; Hampel, C.; Werner, H.-J. *J. Chem. Phys.* **1993**, *99*, 5129.

(39) MOLPRO is a package of ab initio programs written by H.-J. Werner and P. J. Knowles with contributions from R. D. Amos, A. Bernhardsson, A. Berning, P. Celani, D. L. Cooper, M. J. O. Deegan, A. J. Dobbyn, F. Eckert, C. Hampel, G. Hetzer, T. Korona, R. Lindh, A. W. Lloyd, S. J. McNicholas, F. R. Manby, W. Meyer, M. E. Mura, A. Nicklass, P. Palmieri, R. Pitzer, G. Rauhut, M. Schütz, H. Stoll, A. J. Stone, R. Tarroni, and T. Thorsteinsson. Version 2000.1.

(40) Hariharan, P. C.; Pople, J. A. *Theor. Chim. Acta* **1973**, *28*, 213.

(41) Nakano, H. *Chem. Phys. Lett.* **1993**, *207*, 372.

(42) Nakano, H.; Hirao, K.; Gordon, M. S. *J. Chem. Phys.* **1998**, *108*, 5660.

(43) Schmidt, M. W.; Baldridge, K. K.; Boatz, J. A.; Elbert, S. T.; Gordon, M. S.; Jensen, J. H.; Koseki, S.; Matsunaga, N.; Nguyen, K. A.; Su, S. J.; Windus, T. L.; Dupuis, M.; Montgomery, J. A. *J. Comput. Chem.* **1993**, *14*, 1347.

(44) For a more detailed description of the experimental setup, see: Kaiser, R. I. *Chem. Rev.* **2002**, *102*, 1309, and references therein.

(45) Mueller, P. H.; Rondan, N. G.; Houk, K. N.; Harrison, J. F.; Hooper, D.; Willen, B. H.; Liebman, J. F. *J. Am. Chem. Soc.* **1981**, *103*, 5049.

(46) Richards, C. A.; Kim, S.-J.; Yamaguchi, Y.; Schaefer, H. F. *J. Am. Chem. Soc.* **1995**, *117*, 10104.

(47) Sulzbach, H. M.; Bolton, E.; Lenoir, D.; Schleyer, P. v. R.; Schaefer, H. F. *J. Am. Chem. Soc.* **1996**, *118*, 9908.

(48) Armstrong, B. M.; McKee, M. L.; Shevlin, P. B. *J. Am. Chem. Soc.* **1995**, *117*, 3685.

(49) Jones, W.; Boissel, P.; Chiavarino, B.; Crestoni, M. E.; Fornarini, S.; Lamaire, J.; Maitre, P. *Angew. Chem.* **2003**, *115*, 2103; *Angew. Chem., Int. Ed.* **2003**, *42*, 2057.

(50) Solca, N.; Dopfer, O. *Angew. Chem.* **2002**, *114*, 3781; *Angew. Chem., Int. Ed.* **2002**, *41*, 3628.

(51) Schulman, J. M.; Disch, R. L.; Schleyer, P. v. R.; Bühl, M.; Bremer, M.; Koch, W. *J. Am. Chem. Soc.* **1992**, *114*, 7897.

(52) Tsao, M.-L.; Hadad, C. M.; Platz, M. S. *J. Am. Chem. Soc.* **2003**, *125*, 8390.

(53) Basilevsky, M. V. *Chem. Phys.* **1977**, *24*, 81.

(54) Valtazanos, P.; Ruedenberg, K. *Theor. Chim. Acta* **1986**, *69*, 281.

(55) Palmeiro, R.; Frutos, L. M.; Castano, O. *Int. J. Quantum Chem.* **2002**, *86*, 422.

(56) Lasorne, B.; Dive, G.; Lauvergnat, D.; Desouter-Lecomte, M. *J. Chem. Phys.* **2003**, *118*, 5831.

(57) The imaginary vibrational frequency is also obtained when using with the finer integration grid (99 radial shells and 590 angular points per shell).

(58) According to the wave packet dynamic study of Lasorne et al.,[56] the evolution of a system mainly depends on the shape of the wave packet in the entrance valley. With increasing velocity and gradient, the wave packet feels the bifurcating region less and less.

(59) Rablen, P. R.; Hartwig, J. F. *J. Am. Chem. Soc.* **1996**, *118*, 4648.

(60) Borden, W. T.; Davidson, E. R. *Acc. Chem. Res.* **1996**, *29*, 67.

(61) Mebel, A. M.; Lin, M. C.; Yu, T.; Morokuma, K. *J. Phys. Chem. A* **1997**, *101*, 3189.